Monthly Notices
of the
ROYAL ASTRONOMICAL SOCIETY

MNRAS **465,** L99–L103 (2017)
Advance Access publication 2016 October 26

doi:10.1093/mnrasl/slw220

Little evidence for entropy and energy excess beyond r_{500} – an end to ICM pre-heating?

Asif Iqbal,[1⋆] Subhabrata Majumdar,[2⋆] Biman B. Nath,[3] Stefano Ettori,[4,5] Dominique Eckert[6] and Manzoor A. Malik[1⋆]

[1]*Department of Physics, University of Kashmir, Hazratbal, Srinagar, J&K, 190011, India*
[2]*Tata Institute of Fundamental Research, 1 Homi Bhabha Road, Mumbai, 400005, India*
[3]*Raman Research Institute, Sadashiva Nagar, Bangalore, 560080, India*
[4]*INAF, Osservatorio Astronomico di Bologna, Via Ranzani 1, I-40127 Bologna, Italy*
[5]*INFN, Sezione di Bologna, viale Berti Pichat 6/2, I-40127 Bologna, Italy*
[6]*Astronomy Department, University of Geneva 16, ch. d'Ecogia, CH-1290 Versoix, Switzerland*

Accepted 2016 October 20. Received 2016 October 20; in original form 2016 May 30

ABSTRACT

Non-gravitational feedback affects the nature of the intracluster medium (ICM). X-ray cooling of the ICM and *in situ* energy feedback from active galactic nuclei (AGNs) and supernovae as well as pre-heating of the gas at epochs preceding the formation of clusters are proposed mechanisms for such feedback. While cooling and AGN feedbacks are dominant in cluster cores, the signatures of a pre-heated ICM are expected to be present even at large radii. To estimate the degree of pre-heating, with minimum confusion from AGN feedback/cooling, we study the excess entropy and non-gravitational energy profiles up to r_{200} for a sample of 17 galaxy clusters using joint data sets of *Planck* Sunyaev–Zel'dovich pressure and *ROSAT*/Position Sensitive Proportional Counter gas density profiles. The canonical value of pre-heating entropy floor of $\gtrsim$300 keV cm^2, needed in order to match cluster scalings, is ruled out at $\approx 3\sigma$. We also show that the feedback energy of 1 keV particle^{-1} is ruled out at 5.2σ beyond r_{500}. Our analysis takes both non-thermal pressure and clumping into account which can be important in outer regions. Our results based on the direct probe of the ICM in the outermost regions do not support any significant pre-heating.

Key words: galaxies: clusters: intracluster medium – cosmological parameters.

1 INTRODUCTION

Galaxy clusters are the largest and most massive virialized objects in the universe, which makes them ideal probes of the large-scale structure of the universe and hence of cosmological parameters that govern the growth of structures (see Gladders et al. 2007 and references therein). However, in order to obtain robust estimates of these parameters, using X-ray techniques, one requires precise knowledge about the evolution of galaxy clusters with redshift and the thermodynamical properties of intracluster medium (ICM). In the simplest case, where one considers pure gravitational collapse, cluster scaling relations are expected to follow self-similarity (Kaiser 1986; Sereno & Ettori 2015). X-ray scaling relations have been widely used to test the strength of correlations between cluster properties and to probe the extent of self-similarity of clusters (Morandi, Ettori & Moscardini 2007). These observations show departure from self-similarity; for example, the luminosity–temperature (L_x–T) relation for self-similar models predicts a shallower slope ($L_x \propto T^2$) than observed ($L_x \propto T^3$). Similarly, Sunyaev–Zel'dovich (SZ) scaling relations also show similar departure (Holder & Carlstrom 2001).

Such departures point towards the importance of complex non-gravitational processes over and above the shock heating of the ICM. The first idea aimed at explaining departure from self-similar scaling relations is that of pre-heating, first proposed by Kaiser (1991) and later extended by others (Evrard & Henry 1991; Babul et al. 2002). In this scenario, the cluster forms from an already pre-heated and enriched gas due to feedback processes (such as galactic winds or active galctic nucleus, AGN) heating up the surrounding gas at high redshifts. Pre-heating models require constant entropy level of $\gtrsim$300 keV cm^2 in order to explain the break in the self-similarity scaling relations (Tozzi & Norman 2001; Babul et al. 2002; McCarthy, Babul & Balogh 2002). In terms of ICM energetics, this typically translates into feedback energy of $\sim$1 keV per particle (Tozzi & Norman 2001; Pipino et al. 2002; Finoguenov et al. 2003). However, there is an ambiguity in defining pre-heating energy/particle since it depends on the density at which gas is heated (less dense gas requires smaller energy to raise it to a particular entropic state). Therefore, pre-heating is best expressed in terms of entropy.

⋆ E-mail: asifiqbal@kashmiruniversity.net (AI); subha@tifr.res.in (SM); mmalik@kashmiruniversity.ac.in (MAM)

Although, early pre-heating models could describe the scaling relations in clusters, it had drawbacks with regard to details. For example, these models predicted isentropic cores particularly in the low-mass clusters (Ponman et al. 2003) and an excess of entropy in the outskirts of the clusters (Voit et al. 2003) which are not consistent with observations. The idea of pre-heating has endured and has found resurgence in recent times (see Pfrommer et al. 2012; Lu et al. 2015 and references therein). Pfrommer et al. (2012) suggested time-dependent entropy injection due to tera electron volt blazars which provide uniform heat at $z \sim 3.5$ peaking near $z \sim 1$ and subsequent formation of cool core (CC) clusters by early forming groups and non-cool core (NCC) clusters by late forming groups, while Lu et al. (2015) explored preventative scenario of feedback in which the circum-halo medium is heated to finite entropy.

In contrast to pre-heating, there can also be *in situ* effects such as injection of energy feedback from AGN, radiative cooling, supernovae and star formation, influencing the thermal structure of ICM (Roychowdhury et al. 2005; Pratt et al. 2010; Eckert et al. 2013a). There is growing evidence that AGN feedback mechanism provides a major source of heating for the ICM (McNamara & Nulsen 2007; Fabian 2012; Chaudhuri, Majumdar & Nath 2013) in the cluster cores. Outside cluster cores, however, the estimates of entropy floor and feedback energy (particularly in massive clusters) are more reflective of pre-heating of gas since (i) the effect of central sources is unlikely to be significant and (ii) the loss of energy through radiation is negligible.

It is worth noting that irrespective of the nature of feedback, the thermodynamic history of the ICM is fully encoded in the entropy of the ICM. The ICM entropy profile is defined as[1] $K(r) = k_{\rm B} T n_{\rm e}(r)^{-2/3}$, where $k_{\rm B}$ is the Boltzmann constant. Non-radiative adaptive mesh refinement (AMR)/smoothed particle hydrodynamics (SPH) simulations, which encodes only gravitational/shock heating, predict entropy profiles of the form $K(r) \propto r^{1.1}$ (Voit, Kay & Bryan 2005). Apart from slightly larger normalization, it has been found that there is significantly higher (flatter) core entropy in AMR case as a result of the hydrodynamical processes that are resolved in the code (e.g. shocks and mixing motions) (Mitchell et al. 2009; Vazza 2011; Power, Read & Hobbs 2014). On the other hand, observations find deviations from the predicted entropy profile at small radii (Pratt et al. 2010; Eckert et al. 2013a) as well as large radii (Eckert et al. 2013a; Su et al. 2015).

A meaningful comparison of recent observations with theoretically expected entropy profiles can thus be used to determine the nature and degree of feedback. This idea was developed and used recently by Chaudhuri, Nath & Majumdar (2012) and Chaudhuri et al. (2013) who estimated the non-gravitational energy deposition profile in the cluster cores. They compared benchmark non-radiative AMR/SPH entropy profiles (Voit et al. 2005) with observed entropy profiles for the REXCESS sample of 31 clusters (Pratt et al. 2010) and found the excess mean energy per particle to be $\sim$1.6–2.7 keV up to r_{500}. Further, they showed that the excess energy is strongly correlated with AGN feedback in cluster cores (Chaudhuri et al. 2013).

In this study, we extend their work by going beyond r_{500} and estimate entropy floor and feedback energetics at large cluster radii. The effect of clumping and non-thermal pressure, especially at large radii, has been shown to be important (Shaw et al. 2010; Battaglia et al. 2015; Eckert et al. 2015; Shi et al. 2015) and we incorporate both in our analysis.

We study the joint data set of *Planck* SZ pressure profiles and *ROSAT* gas density profiles of 17 clusters (Eckert et al. 2012; Planck Collaboration V 2013) to estimate entropy profiles up to r_{200} and beyond.[2] As detailed in Eckert et al. (2013a), we use the parametric profiles which are obtained by fitting a functional form to projected emission-measure density and *Planck* SZ pressure data (Vikhlinin et al. 2006; Nagai, Kravtsov & Vikhlinin 2007).[3] The parametric profiles have less cluster-to-cluster scatter and errors; however, they are consistent with the non-parametric deprojected profiles. Below $0.2\,r_{500}$, the resolution of both *Planck* and *ROSAT* is insufficient to obtain reliable constraints.

In the last 25 yr since its proposal, the evidence for-or-against pre-heating has been mainly circumstantial. In this Letter, we show that a direct estimate of entropy floor and non-gravitational energy in the outer regions is insignificant enough so as to rule out pre-heating scenarios. Throughout this work, we will assume $(\Omega_{\rm m}, \Omega_\Lambda, h_0) = (0.3, 0.7, 0.7)$.

2 ANALYSIS

2.1 Cluster modelling

The total hydrostatic mass profile $M(r)$ of the galaxy clusters is given by $M(r) = -\frac{r^2}{G\rho_{\rm g}(r)} \frac{{\rm d}P_{\rm g}(r)}{{\rm d}r}$, where $\rho_{\rm g}$ and $P_{\rm g}$ are the parametric forms of the density and thermal pressure of the ICM, respectively (Eckert et al. 2013a; Planck Collaboration V 2013). The radii r_{500} and r_{200} are obtained by first interpolating the $M(r)$ profile and then iteratively solving[4] for $m_\Delta = (4/3)\, r_\Delta^3\, \Delta\, \rho_{\rm c}(z)$. The virial radius, $r_{\rm vir}(M_{\rm vir}, z)$, is calculated with spherical collapse model $r_{\rm vir} = \left[\frac{M_{\rm vir}}{4\pi/3 \Delta_{\rm c}(z) \rho_{\rm c}(z)}\right]^{1/3}$, where $\Delta_{\rm c}(z) = 18\pi^2 + 82(\Omega_{\rm m}(z) - 1) - 39(\Omega_{\rm m}(z) - 1)^2$. If required, virial radius is obtained by linear extrapolation of mass profile in logarithmic space.

Since the 'actual' total mass is also partially supported by non-thermal pressure, we model the non-thermal pressure fraction using the form given in Shaw et al. (2010),

$$P_{\rm nt}(r, z) = f(r, z)\, P_{\rm tot} = \frac{f(r, z)}{1 + f(r, z)}\, P_{\rm g}(r), \quad (1)$$

where $P_{\rm tot}$ is total gas pressure, $f(r, z) = a(z) \left(\frac{r}{r_{500}}\right)^{n_{\rm nt}}$, $a(z) = a_0(1 + z)^\beta$ with $a_0 = 0.18 \pm 0.06$, $\beta = 0.5$ and $n_{\rm nt} = 0.8 \pm 0.25$ (Shaw et al. 2010). We also study the effect of different non-thermal pressure fraction by varying a_0. For our sample, the fiducial $P_{\rm nt}$ is $\sim$50 per cent of the thermal gas pressure, $P_{\rm g}$, around $r_{\rm vir}$ and corresponds to a mass difference of the order of 20 per cent at r_{500}. This is in good agreement with simulations/theoretical predictions (Shi et al. 2015). The value of r_{500} obtained from the resultant mass profiles are consistent with the Planck Collaboration XI (2011). With the addition of the non-thermal pressure, the value of r_{500} typically

[1] Thermodynamic definition of specific entropy being $S = \ln K^{3/2} +$ constant.

[2] We have left out cluster 'A2163' from Eckert et al. (2013a,b) in this work as its estimated feedback profile was found hugely different from others. This cluster is in the perturbed state and presumably out of hydrostatic equilibrium (Soucail 2012).

[3] www.isdc.unige.ch/~deckert/newsite/Dominique_Eckerts_Homepage.html.

[4] Δ is defined such that r_Δ is the radius out to which the mean matter density is $\Delta\rho_{\rm c}$, where $\rho_{\rm c} = 3H^2(z)/8\pi G$ being critical density of the universe at redshift z.

increases by 50–150 Kpc; however, this difference is degenerate with the value of the normalization of $P_{\rm nt}$.

2.2 Initial entropy profile

Models of the formation of the large-scale structure, where gas is shock heated as it falls in the cluster dark matter potential well, predict that the gas entropy $K_{\rm th}(r)$ has a power-law behaviour with radius outside of cluster cores. For non-radiative AMR simulations, Voit et al. (2005) entropy profile is well described in the range (0.2–1) r_{200} by

$$\frac{K_{\rm th}(r)}{K_{200}} = 1.41 \left(\frac{r}{r_{200}}\right)^{1.1}, \quad (2)$$

plus a flatter core below $0.2\,r_{200}$ with $K_{200} = 144(\frac{m_{200}}{10^{14}\,{\rm M}_\odot})^{2/3}(\frac{1}{f_{\rm b}})^{2/3}h(z)^{-2/3}$ keV cm^2. We fix $f_{\rm b} = 0.156$ from the recent *Planck* results (Planck Collaboration XVI 2013). It has been found that the entropy profiles after taking cooling into account differ with equation (2) significant only up 300 Kpc for 10^{15} solar mass cluster (McCarthy et al. 2008) which corresponds to $\approx 0.2\,r_{500} \approx 0.1\,m_{\rm g}/m_{\rm g,\,500}$ for our sample.

The hydrostatic equation, now including both thermal and non-thermal pressure, can be rewritten in terms of the entropy as

$$\frac{{\rm d}(P_{\rm g} + P_{\rm nt})}{{\rm d}r} = -\left(\frac{P_{\rm g}}{K_{\rm th}}\right)^{3/5} m_{\rm p}\mu_{\rm e}^{2/5}\,\mu^{3/5}\,\frac{GM_{\rm tot}(<r)}{r^2}, \quad (3)$$

where $M_{\rm tot}$ is the total mass which is equated to $M_{\rm thermal} + M_{\rm non\text{-}thermal}$. For boundary condition, we fix the gas fraction ($f_{\rm g}$) to be $0.9 f_{\rm b}$ at virial radius (Crain et al. 2007). Initial profiles for density and temperature are found using equations (2) & (3).

Recently, both simulations and observations have found significant clumping beyond r_{500}, which, by definition, is measured as $C = <\rho_{\rm g}^2>/<\rho_{\rm g}>^2$ (Eckert et al. 2013a, 2015; Battaglia et al. 2015). Eckert et al. (2015) found azimuthal median is a good tracer of the true 3D density (clumping factor) and showed from both hydrodynamical simulations and synthetic simulations that their method recovered the true 3D density profiles with deviations less than 10 per cent at all radii. They found that the average $\sqrt{C} = 1.25$ at r_{200}, consistent with the numerical simulations. Since clumping in the ICM is a plausible reason for the observed flattening of the entropy profiles in the outer regions, we estimate the observed entropy profiles by incorporating clumping using the recent parametric form of the clumping profile given in section 4.1 of Eckert et al. (2015).

2.3 Estimates of total feedback energy

To estimate the feedback thermal energy, we need to relate the entropy change (i.e. $\Delta K = K_{\rm obs} - K_{\rm th}$) with change in energy. Considering isobaric approximation, thermal energy change per unit mass is given by $\Delta Q = \frac{kT_{\rm obs}}{(1-\frac{1}{\gamma})\mu m_{\rm p}} \frac{\beta^{2/3}(\beta-1)}{(\beta^{5/3}-1)} \frac{\Delta K}{K_{\rm obs}}$ (see Chaudhuri et al. 2012 for details), where $\beta = T_{\rm obs}/T_{\rm th}$ and $\gamma = 5/3$. Most importantly, in order to take into account the redistribution of gas mass due to the feedback, one should compare entropy profiles for the same enclosed gas mass (i.e. $\Delta K(m_{\rm g})$) instead at the same radii ($\Delta K(r)$) as commonly done in the literature (Li et al. 2011; Nath & Majumdar 2011; Chaudhuri et al. 2012, 2013). The corresponding mechanical feedback energy per particle '$\Delta E_{\rm ICM}$' can be written in terms of change in thermal and potential energies as

$$\Delta E_{\rm ICM} = \mu m_{\rm p}\Delta Q + G\mu m_{\rm p}\left(\frac{M_{\rm tot}(r_{\rm th})}{r_{\rm th}} - \frac{M_{\rm tot}(r_{\rm obs})}{r_{\rm obs}}\right), \quad (4)$$

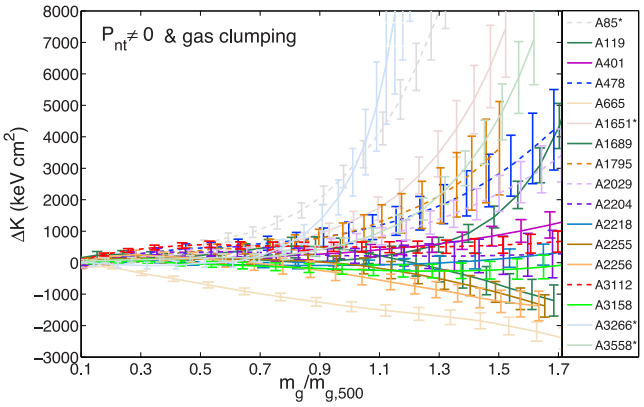

Figure 1. The excess entropy ΔK as a function of $m_{\rm g}/m_{\rm g,500}$ for all clusters. Solid and dashed lines represent NCC and CC clusters, respectively. Four clusters marked with $*$ have large value of ΔK (>4000 keV cm^2) in outer regions and are not included in the sub-sample (see Table 1). The error bars are given at 1σ level.

where $r_{\rm th}$ and $r_{\rm obs}$ are theoretical and observed radii, respectively, enclosing the same gas mass. The total amount of feedback energy available in the ICM is $E_{\rm ICM} = \int \frac{\Delta E_{\rm ICM}}{\mu m_{\rm p}}\,{\rm d}m_{\rm g}$.

Since clusters lose energy due to X-ray cooling, we estimate total feedback energy deposited in the ICM by adding this lost energy to $E_{\rm ICM}$; thus, $\Delta E_{\rm feedback} = \Delta E_{\rm ICM} + \Delta L_{\rm bol}\,t_{\rm age}$, where $\Delta L_{\rm bol}$ is the bolometric luminosity in a given gas shell which is obtained by using the approximate cooling function Λ_N given by Tozzi & Norman (2001) and $t_{\rm age}$ is the average age of the cluster which we have approximated to be 5 Gyr based on the results of Smith & Taylor (2008). Finally, we estimate the mean non-gravitational energy per particle, $<\Delta E>$, from total energy divided by the total number of particles in the ICM (i.e. $\frac{M_{\rm gas,obs}}{\mu m_{\rm p}}$).

In the rest of the Letter, we refer to the case where the energy lost due to cooling is not added to energy estimated from entropy differences as final (after cooling), i.e. $\Delta E_{\rm ICM}$. In contrast, where the energy lost due to cooling is also added is referred to as initial (before cooling), i.e. $\Delta E_{\rm feedback}$. The latter represents the non-gravitational energy/particle required to heat the gas in a collapsed system from the initial theoretical model to the observed state. However, if the change in configuration is solely due to pre-heating of gas much before the collapse of system then the amount of energy required would be less than $\Delta E_{\rm feedback}$ (McCarthy et al. 2008). This implies that $\Delta E_{\rm feedback}$ represents upper an limit on the pre-heating energy.

3 RESULTS AND DISCUSSION

3.1 Feedback beyond r_{500}

Once the individual profiles are found, we study the mean properties of the sample. The magnitude and profiles of ΔK and ΔE, estimated following the method laid down, provide clue to the feedback on the ICM. In Fig. 1, we show the ΔK profiles for all the 17 clusters. In Fig. 2, we see the weighted average (Louis 1991) ΔK profile is close to 100 keV cm^2 for most of the cluster region. There are four clusters marked with * in Fig. 1, which are not included in the sub-sample for which ΔK profiles have comparatively large value (and hence large positive change in thermal energy) in outer regions. However, after accounting for the change in potential energy along with change in thermal energy, the ΔE profiles for these clusters become close to zero (or even negative).

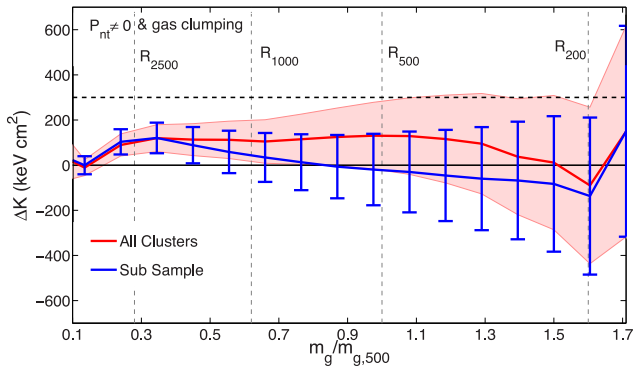

Figure 2. The excess entropy $\Delta K_{\rm feedback}$ as a function of $m_{\rm g}/m_{\rm g,\,500}$. The thick red line shows weighted average profile with 3σ error for the entire sample. Blue line represents average profile for the sub-sample. The vertical dashed lines show the radius of the mean profile for different overdensities. The horizontal black line shows zero entropy and the dashed black line is for $\Delta K_{\rm feedback} = 300$ keV cm^2, indicative of pre-heating.

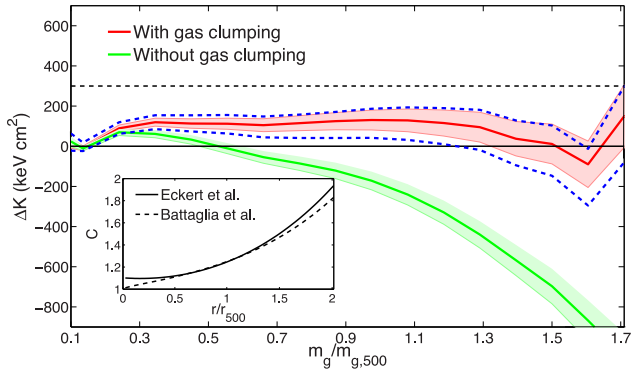

Figure 3. This plot shows the effect on the $\Delta K_{\rm feedback}$ profile by introducing clumping factor using Eckert et al. (2015) best fit. The shaded region shows 1σ error. The region enclosed by two dashed blue lines shows the 1σ error band after accounting for clumping errors (15 per cent of the clumping profile). The inset shows comparison of Eckert et al. (2015) and Battaglia et al. (2015) clumping profiles for the average case.

Moreover, for the sub-sample, $\Delta K = 0$ is always consistent at 1σ beyond r_{1000}. Fig. 3 shows ΔK with and without including clumping in calculations.

In Fig. 4, we show the corresponding average $\Delta E_{\rm feedback}$ (solid red line) for the full sample and compare it with the average of $\Delta E_{\rm ICM}$ (dotted red line). These are indistinguishable beyond $r \sim r_{500}$ since, unlike in the inner region (as explored in Chaudhuri et al. 2013); cooling plays sub-dominant role beyond r_{500}. There is clear evidence of the feedback up to $\approx r_{500}$ with the feedback peaking centrally (also found by Chaudhuri et al. 2013). However, the average ΔE profile is close to zero beyond r_{500}. Since, more than 70 per cent of the cluster volume lies between r_{500}andr_{200}, one can confidently claim insufficient or complete lack of feedback over most of the cluster volume.

3.2 Discussion

It is now amply clear that both non-thermal pressure and clumping are important at large radii. The addition of non-thermal pressure increases the initial entropy profile '$K_{\rm th}(m_{\rm g})$' due to the increase in the normalized K_{200}. This, in turn, leads to the decrease in ΔK and hence ΔE (see Iqbal et al., in preparation for details). Considering

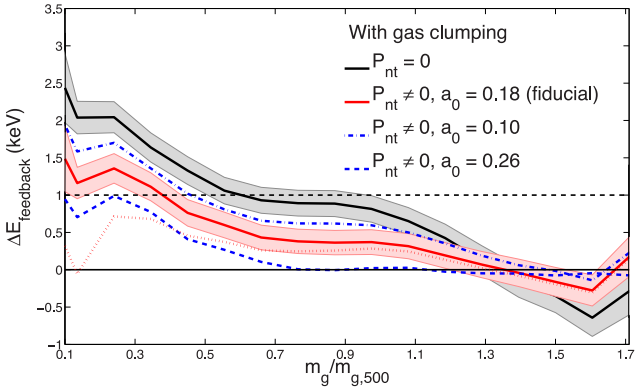

Figure 4. This plot shows the $\Delta E_{\rm feedbck}$ for different normalization a_0 of the non-thermal pressure with larger value of a_0 giving larger non-thermal pressure (see equation 1). We show the 1σ error bands for the fiducial case (i.e. $a_0 = 0.18$, red band) and the purely thermal case (i.e. $a_0 = 0$, grey band). We also show the average profile without adding the energy lost due to cooling (i.e. $\Delta E_{\rm ICM}$) with dotted red line for the fiducial case. For meaningful comparison, we have scaled the x-axis of all the cases with the same $m_{\rm g,\,500}$ as that of fiducial case.

the clumpiness in gas density (and assuming that no fluctuations exist in temperature distribution), however, results in increase in the observed entropy and hence increase in the ΔE. The importance of clumping ($K \sim C^{5/6}$) is highlighted in Fig. 3, where we show the average ΔK profile before and after correcting for the clumping bias. While the estimated entropy excess is unrealistically negative when no correction is applied, it attains a positive value close to zero when the effect of clumping is taken into account following the parametrization of Eckert et al. (2015). Note that this determination is consistent with the expectation of numerical simulations (Battaglia et al. 2015, see the inset of Fig. 3). We find that pre-heating value of entropy floor $\geq$300 keV cm^2 is ruled out at 3σ for the full sample and at 4.2σ for the sub-sample.

To study the impact of non-thermal pressure on the estimate of non-gravitational energy, we show the ΔE profiles for the pure thermal case along with the non-thermal case with three different normalization ($a_0 = 0.10, 0.18, 0.26$) in Fig. 4. These correspond to mass differences of $\sim$(10 per cent, 20 per cent, 30 per cent) at r_{500} for the average profile. The mean excess energy is still far below 1 keV particle^{-1} and consistent with zero beyond a specific radius which depends on the choice of a_0. However, neglecting non-thermal pressure overestimates the feedback energy, though still staying less than 1 keV in the outer regions.

Finally, we list the average energy/particle in Table 1. We find that beyond r_{500}, the $\Delta E_{\rm feedback} = 1$ keV particle^{-1} is ruled out at 5.2σ for the full sample and by 4.8σ for the sub-sample. Since $\Delta E_{\rm feedback}$ is roughly the upper limit of pre-heating energy/particle, this in turn rules out pre-heating scenarios which require 1 keV particle^{-1} to explain the break in scaling relations. At regions below r_{500}, $\Delta E =$ 1 keV particle^{-1} is allowed within 3σ. It may be also noted from the table that our results are insensitive to the choice of the boundary conditions, particularly for the sub-sample. Thus, our constraint on extra heating refers to the inner regions ($<r_{1000}$) only, which strongly corroborate with the results of Gaspari et al. (2014). Our results can be compared to the value obtained by Chaudhuri et al. (2013) who studied the regions inside the core ($r < 0.3r_{500}$) and obtained $1.7 \pm$ 0.9 keV particle^{-1} which they showed to be strongly correlated to the central AGN feedback.[5] The feedback energy left in the ICM is

[5] Note that Chaudhuri et al. (2013) did not consider $P_{\rm nt}$ or clumping.

Table 1. Average feedback energy per ICM particle (in kilo electron volts) after including non-thermal pressure and clumping.

Sample	Final average feedback energy/particle		Initial average feedback energy/particle	
	(0.2–1) r_{500}	r_{500}–r_{200}	(0.2–1) r_{500}	r_{500}–r_{200}
Full sample	0.35 ± 0.17 (0.34 ± 0.17)	0.03 ± 0.18 (0.11 ± 0.17)	0.72 ± 0.17 (0.72 ± 0.17)	0.05 ± 0.18 (0.14 ± 0.17)
Sub-sample	0.60 ± 0.21 (0.60 ± 0.21)	0.11 ± 0.18 (0.11 ± 0.18)	1.00 ± 0.21 (1.00 ± 0.21)	0.13 ± 0.18 (0.13 ± 0.18)

Notes. Columns 2 and 3: average energy per particle in the ranges (0.2–1) r_{500} and r_{500}–r_{200}, respectively, without taking into account energy lost due to cooling (i.e. final feedback energy '$\Delta E_{\rm ICM}$'). Columns 4 and 5: average energy per particle in the ranges (0.2–1) r_{500} and r_{500}–r_{200}, respectively, after taking into account energy lost due to cooling (i.e. initial energy '$\Delta E_{\rm feedback}$'). The numbers in brackets show the average energy per particle for boundary condition $f_{\rm g} = 0.9 f_{\rm b}$ at the last observed radius instead at virial radius. Error bars are given at 1σ level. Clearly, there is little evidence of feedback energy beyond r_{500} for all cases.

much lower for the entire radial range with cooling influencing the average energy per particle mainly in the range pf 0.2–1 r_{500}.

4 CONCLUSIONS

Our analysis shows that the estimated entropy excess and energy input corresponding to this excess of the ICM are much less than required by pre-heating scenarios to explain the break in scaling relations. While the feedback energy estimates rely on some assumptions (isobaric and cooling energy approximations) and refer to energy deposition after the collapse of cluster, the constraints on the ΔK show that pre-heating scenarios that require ΔK more than 300 keV cm^2 can be ruled out. This result holds good whether or not the effects of non-thermal pressure and clumping are taken into account. At large radii, the effect of central sources is unlikely to be significant (Hahn et al. 2015) and the loss of energy through radiation is also negligible. While some previous workers have casted doubts on the simple pre-heating scenario arguing that no single value of energy input can explain the observations (Younger & Bryan 2007), one can, in principle, construct variations in the scenario (Fang & Haiman 2008) in order to explain observations that are dominated by processes in the inner regions. However, our analysis directly probes the entropy floor and energetics of the cluster gas at the outermost regions and shows that any significant pre-heating that can manifest as a property of the ICM is absent.

ACKNOWLEDGEMENTS

This work was supported by SERB (DST) Project Grant No. SR/S2/HEP-29/2012. AI would like to thank TIFR, Mumbai and RRI, Bangalore for hospitality. The project started with discussions when two of the authors (SM and SE) were sharing an office at the Munich Institute for Astro- and Particle Physics (MIAPP) in 2015. SM would like to thank Nick Kaiser and Dick Bond for comments. DTP preprint no. TIFR/TH/16-12. The authors would like to thank the anonymous referees for useful comments that helped in improving the clarity of the manuscript.

REFERENCES

Babul A., Balogh M. L., Lewis G. F., Poole G. B., 2002, MNRAS, 330, 329
Battaglia N., Bond J. R., Pfrommer C., Sievers J. L., 2015, ApJ, 806, 43
Chaudhuri A., Nath B. B., Majumdar S., 2012, ApJ, 759, 5
Chaudhuri A., Majumdar S., Nath B. B., 2013, ApJ, 776, 84
Crain R. A., Eke V. R., Frenk C. S., Jenkins A., McCarthy I. G., Navarro J. F., Pearce F. R., 2007, MNRAS, 377, 41
Eckert D. et al., 2012, A&A, 541, A57
Eckert D., Molendi S., Vazza F., Ettori S., Paltani S., 2013a, A&A, 551, A22
Eckert D., Ettori S., Molendi S., Vazza F., Paltani S., 2013b, A&A, 551, A23
Eckert D., Roncarelli M., Ettori S., Molendi S., Vazza F., Gastaldello F., Rossetti M., 2015, MNRAS, 447, 2198
Evrard A. E., Henry J. P., 1991, ApJ, 383, 95
Fabian A. C., 2012, ARA&A, 50, 455
Fang W., Haiman Z., 2008, ApJ, 680, 200
Finoguenov A., Borgani S., Tornatore L., Böhringer H., 2003, A&A, 398, 35
Gaspari M., Brighenti F., Temi P., Ettori S., 2014, ApJ, 783, L10
Gladders M. D., Yee H. K. C., Majumdar S., Barrientos L. F., Hoekstra H., Hall P. B., Infante L., 2007, ApJ, 655, 128
Hahn O. et al., 2015, MNRAS, preprint (arXiv:1509.04289)
Holder G. P., Carlstrom J. E., 2001, ApJ, 558, 515
Kaiser N., 1986, MNRAS, 222, 323
Kaiser N., 1991, ApJ, 383, 104
Li R., Mo H. J., Fan Z., van den Bosch F. C., Yang X., 2011, MNRAS, 413, 3039
Louis L., 1991, A Practical Guide to Data Analysis for Physical Science Students. Cambridge Univ. Press, Cambridge
Lu Y., Mo H. J., Wechsler R. H., 2015, MNRAS, 446, 1907
McCarthy I. G., Babul A., Balogh M. L., 2002, ApJ, 573, 515
McCarthy I. G., Babul A., Bower R. G., Balogh M. L., 2008, MNRAS, 386, 1309
McNamara B. R., Nulsen P. E. J., 2007, ARA&A, 45, 117
Mitchell N. L., McCarthy I. G., Bower R. G., Theuns T., Crain R. A., 2009, MNRAS, 395, 180
Morandi A., Ettori S., Moscardini L., 2007, MNRAS, 379, 518
Nagai D., Kravtsov A. V., Vikhlinin A., 2007, ApJ, 668, 1
Nath B. B., Majumdar S., 2011, MNRAS, 416, 271
Pfrommer C., Chang P., Broderick A. E., 2012, ApJ, 752, 24
Pipino A., Matteucci F., Borgani S., Biviano A., 2002, New Astron., 7, 227
Planck Collaboration V, 2013, A&A, 550, A131
Planck Collaboration XI, 2011, A&A, 536, A11
Planck Collaboration XVI, 2013, A&A, 571, A20
Ponman T. J., Sanderson A. J. R., Finoguenov A., 2003, MNRAS, 343, 331
Power C., Read J. I., Hobbs A., 2014, MNRAS, 440, 3243
Pratt G. W. et al., 2010, A&A, 511, 14
Roychowdhury S., Ruszkowski M., Nath B. B., 2005, ApJ, 634, 90
Sereno M., Ettori S., 2015, MNRAS, 450, 3675
Shaw L. D., Nagai D., Bhattacharya S., Lau E. T., 2010, ApJ, 725, 1452
Shi X., Komatsu E., Nelson K., Nagai D., 2015, MNRAS, 448, 1020
Smith G. P., Taylor J. E., 2008, ApJ, 682, 73
Soucail G., 2012, A&A, 540, 61
Su Y., Buote D., Gastaldello F., Brighenti F., 2015, ApJ, 805, 104
Tozzi P., Norman C., 2001, ApJ, 546, 63
Vazza F., 2011, MNRAS, 410, 461
Vikhlinin A., Kravtsov A., Forman W., Jones C., Markevitch M., Murray S. S., Van Speybroeck L., 2006, ApJ, 640, 691
Voit G. M., Balogh M. L., Bower R. G., Lacey C. G., Bryan G. L., 2003, ApJ, 593, 272
Voit G. M., Kay S. T., Bryan G. L., 2005, ApJ, 364, 909
Younger J. D., Bryan G. L., 2007, ApJ, 666, 647

This paper has been typeset from a TEX/LATEX file prepared by the author.